TM-82
0423

DC FIELD MEASUREMENTS ON NO. 2 MODEL MAGNET

R. Yamada

September 27, 1968

This is a report of dc field measurements on a new three-foot model bending magnet, which were done mostly in August, 1968. There will be another report of pulsed-field measurements on the same magnet in the near future.

The present dc measurements were done in a situation where we did not have any established equipment. The measuring devices were used as soon as made, while they were being tested. The power supply was not quite satisfactory as far as current regulation and ripple is concerned. We were using a temporary small water tank, which heated up during measurements on hot summer days, and we had to shut off the power and wait until it cooled down.

The present coil of the model has a larger insulation gap in the median plane than we can tolerate, and the inside conductors of the coil are displaced by an amount of 50 mils between top and bottom half coils. We are now designing a better coil for three-foot B2 model magnet.

The environment and the measuring equipment are improving every day so we may have more refined data in the future.

No. 2 Model Magnet

This model is three feet long and made of punched 16-gauge (60-mil thick) laminations. The gap height is two inches and other geometrical dimensions are shown in Figs. 1a and 1b. The laminations are divided into top and bottom halves and the same type of lamination is used.

The top and bottom halves of the magnet were assembled on an assembly jig and bolted together with end plates and four outside bolts. The top and bottom half coils of ten turns each were placed on the respective half iron cores, and these two were put together by other vertical bolts. The two half coils are connected in series. This model magnet was made with the intention that the lamination could be easily changed to test lamination of different materials. Also we can test the crenellation effects at high field and the different end shaping.

The cross section of the lamination is near the final shape. However some further modifications are expected in the final design of the laminations according to the field measurements on model magnets and on the progress of computer calculations.

There are 1.2 in. thick end plates on both ends, and three different types of laminations; 12 in. of ARMCO decarburized iron coated with manganese phosphate, 12 in. USS Vitrenamel 1 with C-5 coating, and 12 in. ARMCO uncoated. The coils were made of the copper conductor which was available at the time of construction; therefore it does

not have most desirable dimensions. The total resistance of the coil is 3.1 mΩ and the inductance is about 2 mH.

The power supply was originally built at LRL, tested and modified here. It is capable of giving 6,000 A at 20 V. It is now still under improvement, and the present current regulation is of the order of 1% with the current ripple of about ± 0.5%.

Measuring Devices

We have recently started to make a fast data acquisition system using a computer, but it is not now available. Most of the measurements reported here were done with a system of search coils, an integrator, a DVM, and human computers.

As is described later we used different types of search coils. The circuit diagram of the integrator is shown in Fig. 2. We used an operational amplifier Model 210 made by Analog Devices, Inc. for the integrator. This operational amplifier uses a solid state chopper and the open loop gain is said about 10^8. But the value of the gain applies for frequencies smaller than 0.1 c/s, and the corresponding gain at the frequency range from 1 to 1000 c/s is about 10^5.

The capacitor is 1 μF polystyrene type, made by Southern Electronics Co. Two potentiometers are used to offset the drift of the integrator and do coarse and fine adjustment. The sensitivity is changed by the selection of the input resistors. Batteries were used for the power supply of the integrator.

The output voltage V_o of the integrator is given by

$$V_o = \frac{NA}{RC} \int \left(\frac{dB}{dt}\right) dt \times 10^{-8}, \text{ volt}$$

$$= \frac{NA}{RC} \left[B\right] \times 10^{-8}, \text{ volt.}$$

With NA = 1000 cm^2, R = 10^3 Ω, C = 10^{-6} F,

$$V_o = \left[B\right] \times 10^{-2}, \text{ volt.} \quad \text{(B in Gauss)}$$

The accuracy we need for gradient measurement is of the order of 0.001 in k (= $\frac{1}{B} \frac{\Delta B}{\Delta x}$, m^{-1}). The corresponding ΔB for B = 10^3 G and Δx = 1 cm is 0.01 G. Then the resolution of the electronic circuit without any amplification should be 100 μV. Therefore the DVM should be capable of reading down to 10 μV.

On the other hand the resolution of the output voltage of the coils should be of the order of 0.1 μV, considering the speed of the probe in the dc magnetic field, e.g., one step/sec.

As we are handling such an extremely low voltage, we have to be careful about any voltage change induced in the search coil lead and in the integrator circuit to reduce drift. It is better to make the length of the leads of search coils and the output cable of the integrator as short as possible.

Also we should reduce the number of the soldered joints and eliminate any unnecessary connectors in these lines to get rid of the effect

of thermocouple voltage. Rough check with a heat gun showed a change of one to five micro-volt for a temperature change of 1° C. That means we should keep all soldered joints and connectors within 1/200 °C during the measurement. Breeze in the room may cause a drift in the output of the integrator. Therefore any joints and connectors, especially ones up to the input of the integrator should be covered and well shielded thermally from the outside.

It seems better if we could have an isolated compartment around the probe and the integrator with air conditioning. Also the surface of the insulators of the integrator should be kept absolutely clean and moisture should be kept to a minimum. For this purpose silica was used inside the chasis. Any soldering in the circuit and wires should be done with a special solder of low thermocouple voltage.

Excitation Curve

The excitation curve of the magnet was measured with a Rawson-Lush rotating coil gaussmeter type 829, which was accurate to 1% in our application. A Bell gaussmeter 620 (Hall probe) was used for a check. The typical excitation curve of ARMCO coated is shown in Fig. 3. The calculated straight line corresponding to a case with infinite permeability is also shown. There is 2% difference between the two curves in the linear region. Finite permeability makes about 1% difference and the remaining 1% error may be due to errors in the

current shunt and the Rawson Probe. We wanted to use an NMR for the absolute calibration, but the ripple and drift of the power supply was too big to allow any measurements.

There is no saturation effect in excitation curve up to 15.5 kG. The ratio of the actual current for a certain field value to the calculated one from the extension of the initial linear region is called Amp factor. The respective Amp factors for different irons are shown in Table I where the maximum error for Amp factors is ± 0.02.

The slope of the initial linear regions of excitation curves is almost the same for different irons, but the saturation effect given by Amp factor is quite different. The coated ARMCO has the extra process of coating on it, but shows less saturation, contrary to our expectation. This seems to be due to the variation of stacking factor along the magnet, as can be seen from the measured values of stacking factor shown in Table I.

Table I. Amp Factor of Different Irons Used in Model Magnet No. 2

	ARMCO Coated	USS Vit. 1	ARMCO Uncoated
18 kG	1.045	1.04	1.055
20 kG	1.095	1.09	1.115
22.5 kG	1.24	1.24	1.285
Stacking Factor (%)	96.3	94.9	92.9

The stacking factor is measured from the calculated overall volume, the total weight, and the densities of the irons. The actual density of each iron was measured using a precision balance with 0.1 mg resolution and a pyconometer. The weight of the following items are measured for the calculation of the iron density, the pyconometer alone, the pyconometer plus iron sample in it, the pyconometer plus iron sample filled with pure water, and the pyconometer filled with pure water. The density of the water as a function of temperature was obtained from the handbook of chemistry and physics.

Remanent Field

The magnet has been excited up to 23 kG, and the remanent field was measured with a Hall probe, Bell Gaussmeter 620, and a DVM. Also the remanent field was measured by a search coil and an integrator, using a flipper which rotates the search coil 180 degrees. For the excitation of 9 kG corresponding to 200 BeV, the remanent field may be about two thirds of what we have measured at 23 kG.

The remanent field on the center line along the magnet is shown in Fig. 4. The measurement did not cover the whole length of the magnet due to the shortness of the probe length. It shows the remanent field of the ARMCO irons is about 11 to 12 G, while that of the USS iron seems about 25 G. This can be explained from the measured values of the coercive forces of 1.09 and 2.44 oersted for ARMCO and USS

respectively,[1] and the ratio of about 10 between the gap height and the magnetic path length in iron. The bump at the end is due to the end plate of SAE 1010 iron.

The radial distributions of the remanent field corresponding to three irons are shown in Fig. 5. All curves are convex at the center, which may be due to the longer magnetic path length at the center, and also due to the fact that iron surface outside the gap region is less excited and having less surface magnetic charge. These curves are normalized at central values and their field shapes are shown in Fig. 6. The USS iron has a bigger remanent field and also a bigger sextupole term.

Gradient Distribution

The gradients were measured with twin coils and an integrator.[2,3] The dimensions of the coils (L2-L3) are shown in Fig. 7. No. 36 gauge wire (5 mil ϕ) was wound about 428 turns each. The total resistance of twin coils is 140 Ω. The twin coils were matched to each other with an accuracy of 2×10^{-5}. To match twin coils they were connected to buck each other and placed in the almost uniform field of the model magnet. The magnet was excited on and off to read the difference of them. The area of a loop on the top of one coil was adjusted to obtain the matching.

The present system of search coils and the integrator works fairly well for the gradient measurement at high field. But it has a considerable drift at low field around injection field. Therefore each point in the gap

was measured successively in one direction and then in the other direction. The average of these two measurements were relatively free from drift, because the observed drift was linear in time in most cases. Several cases were tested with different magnitudes of drift, and it was found that fairly large linear drift can be corrected in this way.

Search coils with a bigger turn-area using finer wires and a better integrator with less drift are being developed.

The first several measurements were the average of both orientations of the twin coils to cancel the remaining mismatching of the coils.[2] But the difference in their shapes were almost negligible. Therefore the most measurements were done with one orientation of the coils. The absolute value k(o) at the center of the magnet was derived from the average of two measurements at center corresponding to two orientations of the twin coils. The estimated error of k(o) is about ± 0.002, which seems to be studied more carefully.

The measured k (= $dB/dx \cdot 1/B$ in m^{-1}) values are shown in Fig. 7, 8, and 9, for each iron. The related values observed from Epstein Square[1] and dimensions of the coil conductors are also included. The curves for USS iron show quite a difference from ARMCO irons at low field and also at high field.

A. Injection Field and Low Field

As expected from the remanent field distribution, USS iron shows a stronger sextupole term at injection field than ARMCO irons. The

values of the measured sextupole term are shown in Table II. Also the expected values from the remanent field shapes are shown. These values were estimated from the assumption that the injection field is a superposition of the remanent field and a field determined by the geometry of iron core and copper conductors.

Table II. Sextupole Term $\frac{1}{B}\frac{d^2B}{dx^2}$ (m^{-2})

USS	kG	Measured Values	Expected Values
USS	0.5	1.8	1.8
USS	1.0	1.1	0.9
ARMCO uncoated	0.5	0.42	0.4
ARMCO uncoated	1.0	0.36	0.2
ARMCO coated	0.5	0.76	0.5
ARMCO coated	1.0	0.31	0.25

Both measured and expected values agree fairly well with each other. The discrepancy in some cases may be due to a drift in the integrator circuit.

The usable region, within $k = \pm 0.02$, corresponding to a ν-shift of 0.25, is almost as wide as that of high field for ARMCO irons. The usable region of USS iron is very narrow, and needs a correction system. It seems iron with a coercive force of 1 oersted seems very desirable from this data. Variation of $\pm 10\%$ in coercive force may be tolerable.

Especially with USS iron, the difference between the low field distribution and the intermediate one is reduced inversely proportionally to the magnitude of the field value.

B. Intermediate Field Up to 20 kG

Up to 18 kG (= 400 BeV), there is no appreciable change due to saturation in gradient distribution. With ARMCO iron this seems true up to 20 kG.

The usable region is about ± 1.3 in., which may actually extend further by about 0.2 in. due to the finite dimensions of twin coils (the width of the twin coils is 0.375 in. each and they are glued together as shown in Fig. 7). The usable region is slightly wider at 18 kG than at 9 kG.

The droop of the field shapes beyond ± 1.3 in. is mainly due to the finite thickness of the insulation gap of about 180 mils in the median plane.[3] Recently F. C. Shoemaker calculated the effects of insulation gaps and conductor holes, and his result agreed fairly well with the measured values on median plane.[4] The present magnet coil is divided into top and bottom halves, but a new coil is planned to be made into one unit to reduce the median plane insulation gap. Then the usable region is expected to be wider.

C. High Field Above 20 kG

The two ARMCO irons show a similar tendency, while USS iron has a bigger saturation effect. This effect comes from the fact that

above the saturation point of iron the field due to the coil starts affecting the field shape in the gap. Therefore the field near the coil gets bigger and eventually the magnetic field shows a concave pattern at center.

The saturation point seems a little low for USS iron compared to ARMCO irons, as can be seen from the accompanying Epstein data (B and μ values may be reduced by a few per cent in a future calibration, but not H_c).[1]

To compensate the saturation effect it is planned to crenellate the lamination or punch a hole in it.

D. Off the Median Plane

The gradient was also measured off the median plane. Examples at 250 and 450 mils above the median plane are shown in Fig. 10, which was measured at 9 kG with ARMCO coated iron and normalized to zero at center.

The distributions were found later not summetrical about the median plane, and seem sensitive to the displacement of the inner surfaces of the top and bottom copper conductors. In our case it is about 40 mils. Recently this effect was also calculated by F. C. Shoemaker and the calculation seems to agree well with measurements. The tolerance of this displacement should be set.

End Field

There are 1.2 in. thick end plates made of hot rolled (SAE 1010)

iron on both ends. The two ends of this model magnet are tapered differently from each other as shown in Fig. 1b.

The field distribution along the center was measured with a small point coil, which was bucked by another fixed identical coil to reduce drift especially in the homogeneous region. The field distributions at 9 and 18 kG are shown in Figs. 11 and 12 for each case. The one at injection was measured with Hall probe and shown in Fig. 11.

The two-step tapered end shows less chance for a change of 9 kG to 18 kG. The effective magnetic length was numerically calculated in these cases and found as shown in Table III, where the negative values correspond to positions outside the edge of the magnet iron. The effective magnetic length was also checked by a method of long coils, which covered the total fringing field.[2]

Table III. Magnetic Length of End Field

Type	0.5 kG	9 kG	18 kG	Difference between 9 and 18 kG
45°	------	-0.92"	-0.82"	0.10"
2-step tapered	-0.51"	-0.45"	-0.40"	0.05"

The radial distribution of the magnetic length was measured for the two-step tapered end. A 20 in. long coil, which is homogeneously wound along the length, is used. Another 20 in. bucking long coil is placed at the other end, and its position is adjusted until its signal cancels the other signal almost completely. Then the former coil is moved across the gap perpendicularly to measure small change in the magnetic length.

The results are shown in Fig. 13 where the curves are normalized at center. At 9 and 18 kG the distributions show a convex curve which corresponds to a change of 0.009 in k at ± 1 inch, considering two end fields for a magnet length of 20 feet. This value seems big enough so that we need more complicated end shaping. But at 22.5 kG, the distribution gets almost uniform due to a balance between the saturation of iron and the field determined by the coil.

Back Leg and Gap Height

The gap in the back legs were measured with the Hall probe.[2] The sensitive element is held 0.4 in. from the iron. The distribution of the gap on both sides of the magnet is shown in Fig. 14. The measurement was done at the excitation of 9 kG which is free from leakage flux due to saturation.

A difference of 1 mil between two gaps on both sides causes an inclination of one twenty-fifth mil/in. This causes the deviation of k(o) at center by 0.008/m for the gap of 2 in. Therefore if we allow the maximum permissible error of ± 0.002 in k(o), the maximum allowable variation in the back leg gaps is ± 2.5 mils and the maximum inclination on the pole surface is ± 0.1 mil/in.

The gap height in the main gap was measured with a dial gauge fixed on a base three and a half inches long which was slid on the lower surface of the gap. Some laminations were sticking up or down locally by an amount of ± 2 mils. Therefore we read the average reading over

three inches on the center line and at ± 1.25 in. off the center. The values are shown in Fig. 15.

Homogeneity

The central field along the magnet was measured at several different excitation levels. At 9 kG, the field is uniform within ± 0.06%. But it shows quite a variation at 22.5 kG due to the three different irons, as expected from the difference in excitation curves. The injection field shows a big variation of ± 1.5% due to the difference in the remanent field, but the variation within the same iron seems less than ± 0.25%.

For high fields two identical point coils were used as a moving coil and a standard coil, which were connected in series to buck each other for the elimination of current variation effect. The Hall probe was used for the injection field.

Acknowledgments

The measurements reported here could not have been done without great assistance from Dr. E. I. Malamud, Dr. J. F. Schivell, and Mr. H. K. Feng. Many of the technical staff in the Cidair Building greatly contributed in different phases of the measurements, including electronics, search coils, the power supply, setting up and also participating in measurements.

REFERENCES

[1] To be reported in a separate report.

[2] R. Yamada and S. Mori, Cornell 10 GeV Synchrotron Report CS-31, April 27, 1966; R. Yamada, CS-36, January 12, 1968.

[3] R. Yamada, E. C. Berrill, T. W. Hardek, and R. S. Odwazny, NAL Internal Report FN-110, January 9, 1968.

[4] Private communication and to be reported in the future.

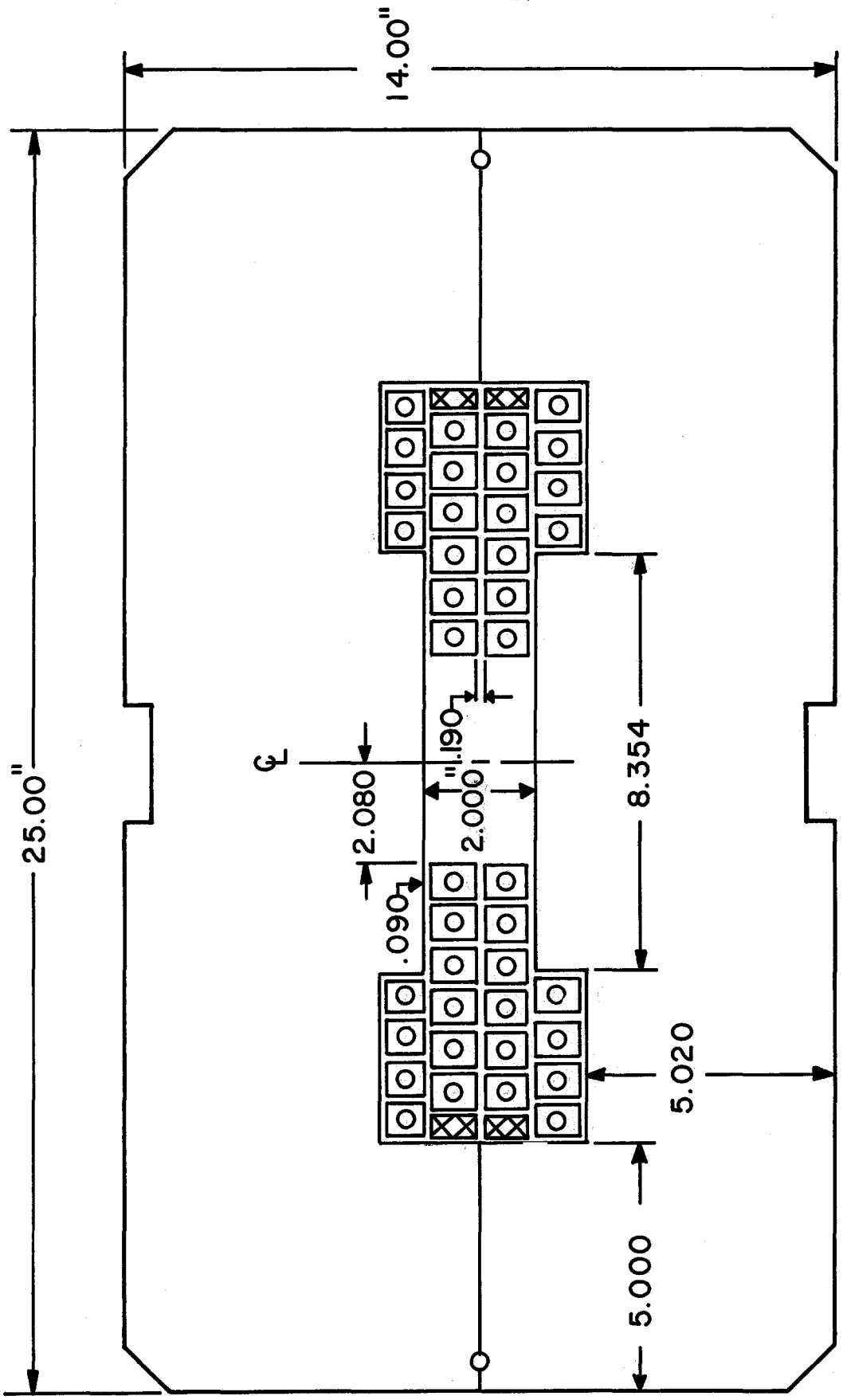

Figure Ia Front Cross Section of Model Magnet No. 2

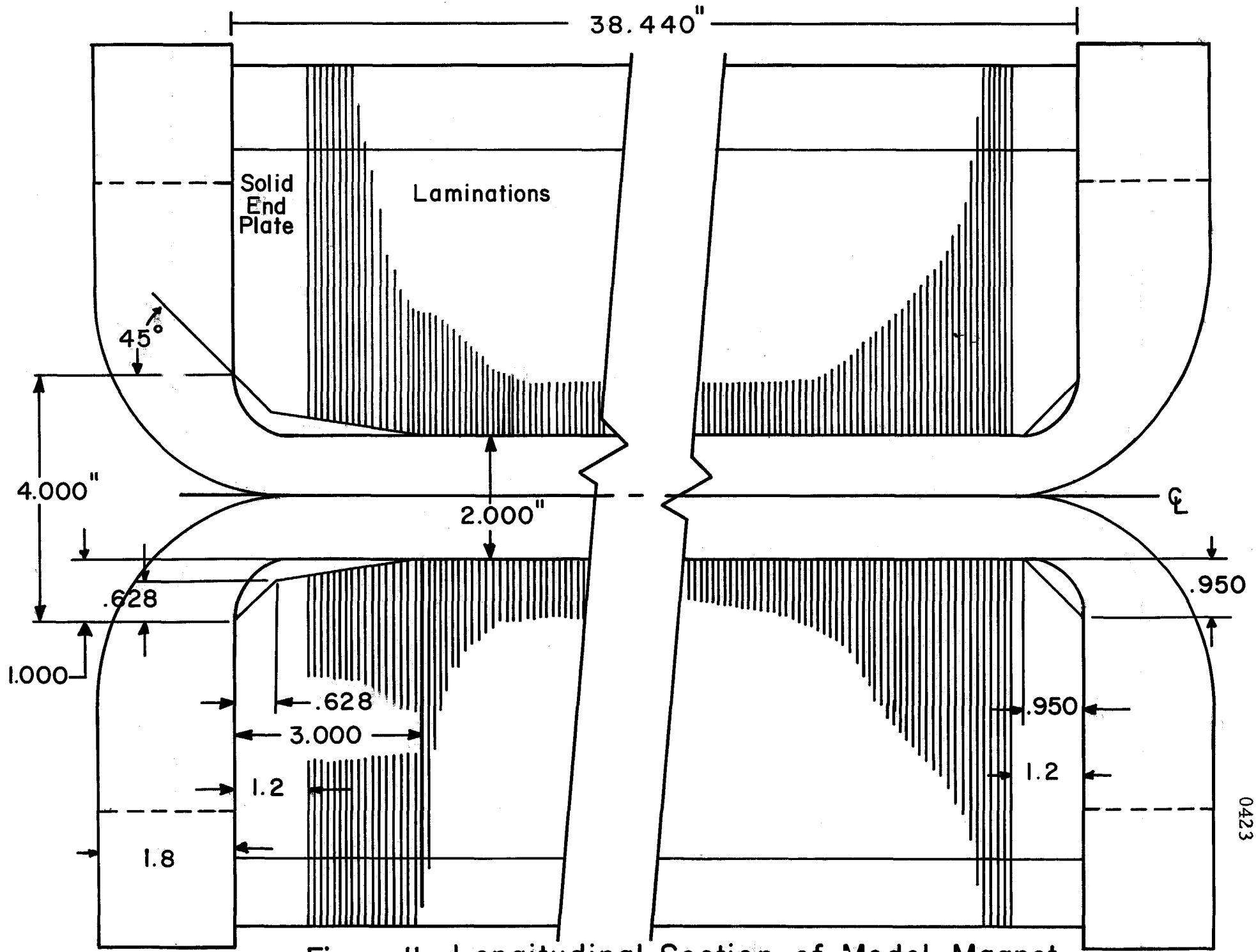

Figure Ib Longitudinal Section of Model Magnet No. 2

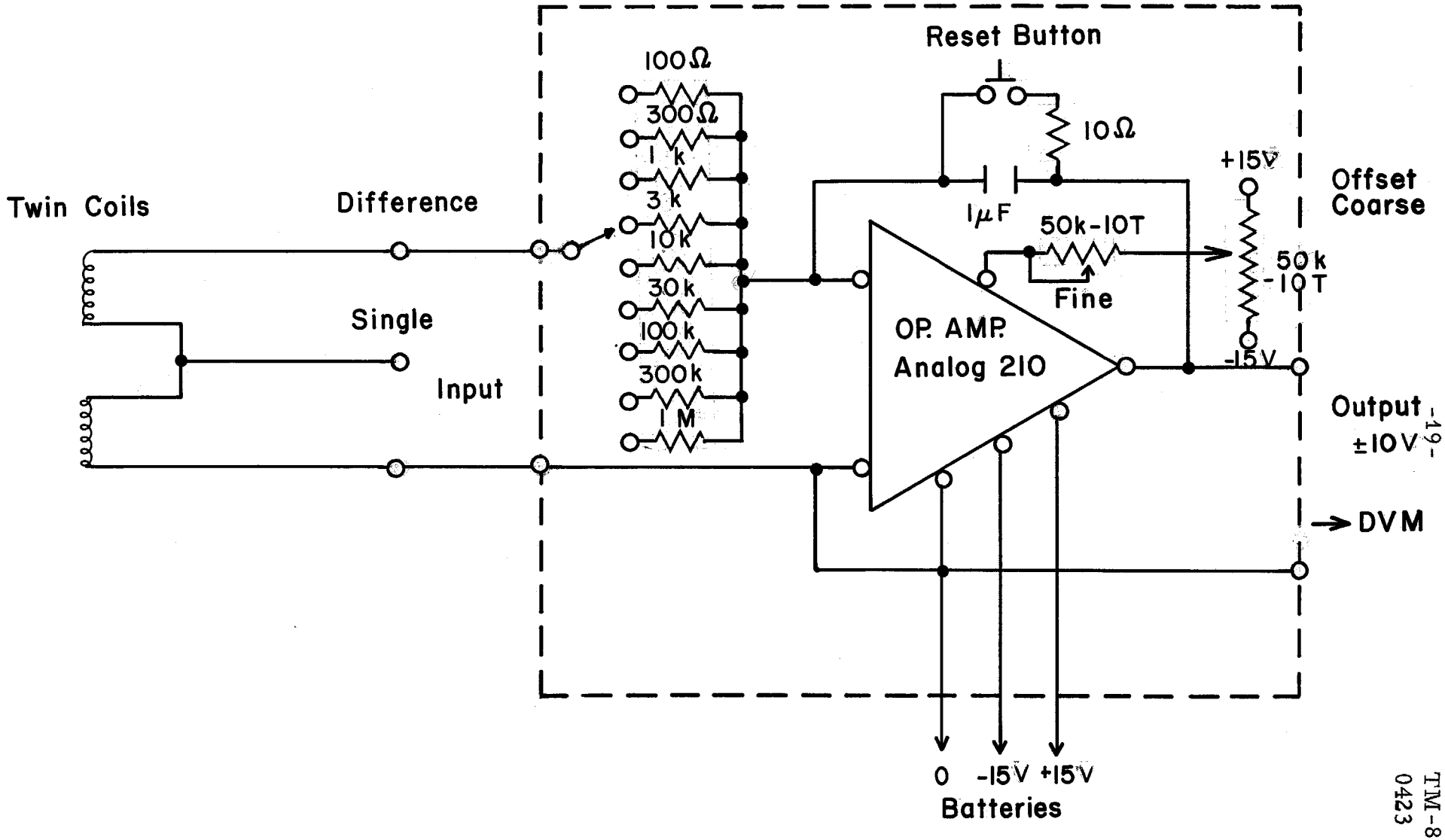

Figure 2 Circuit Diagram

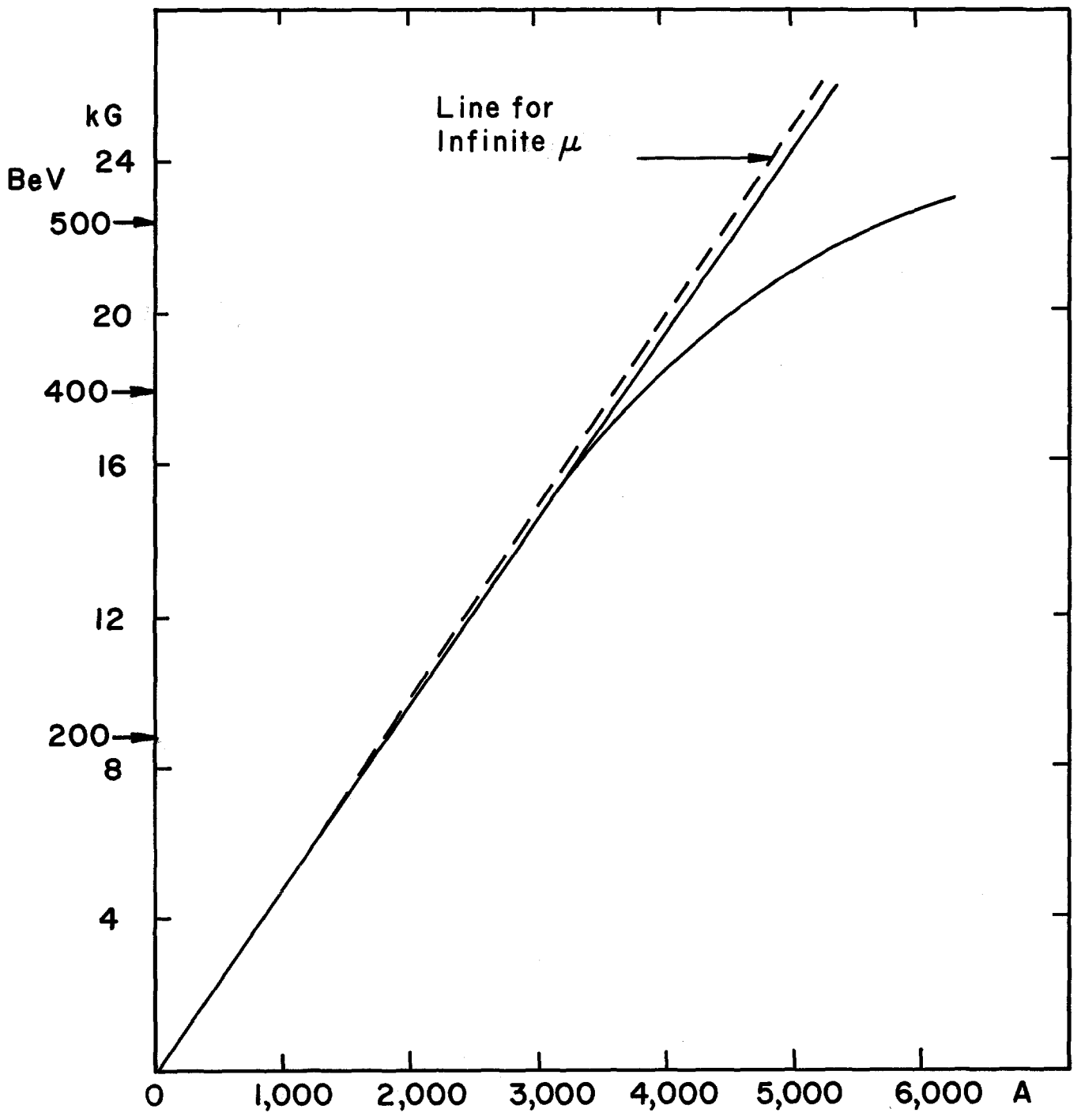

Figure 3 Excitation Curve of Armco Coated

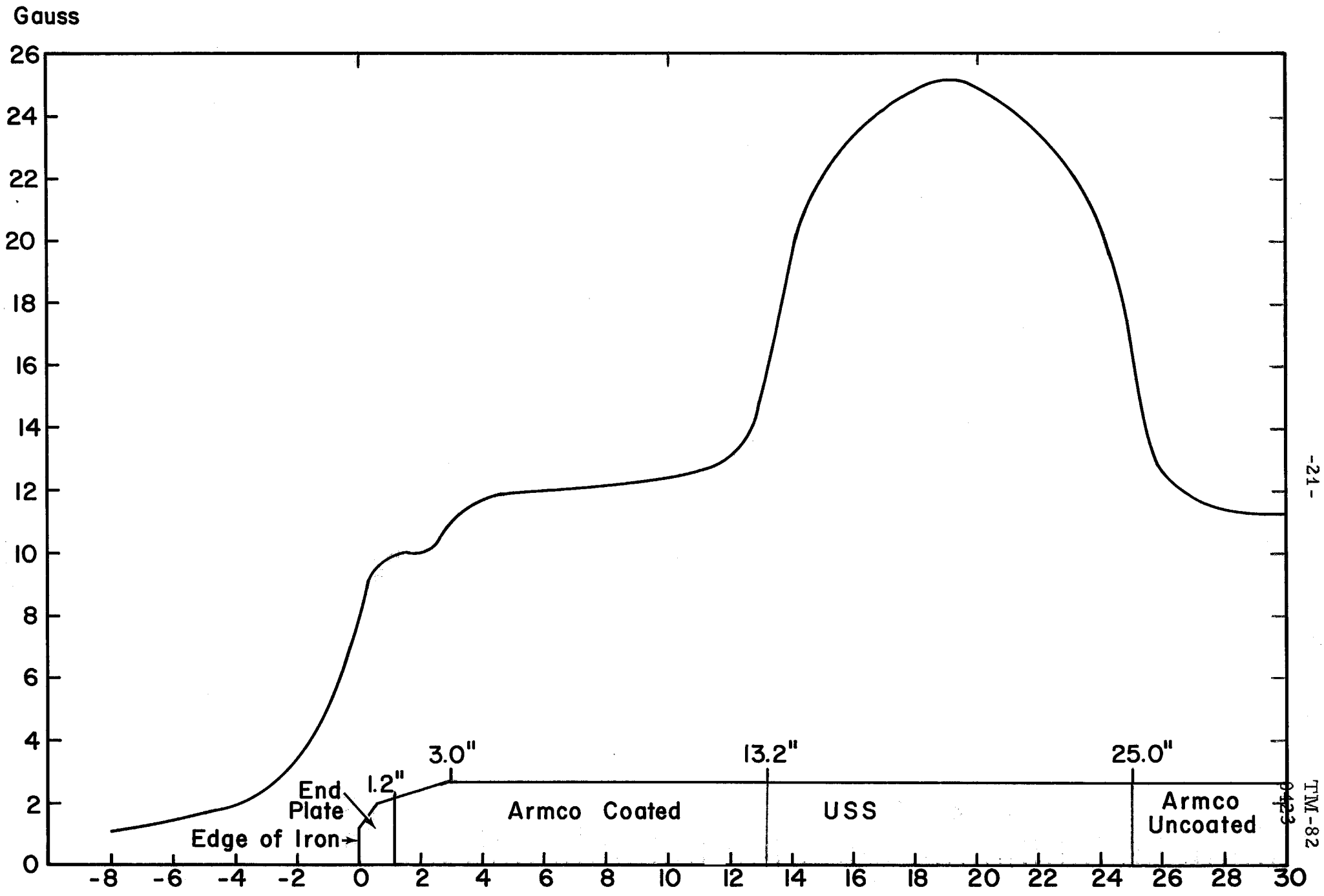

Figure 4 Remanent Field Along Center Line

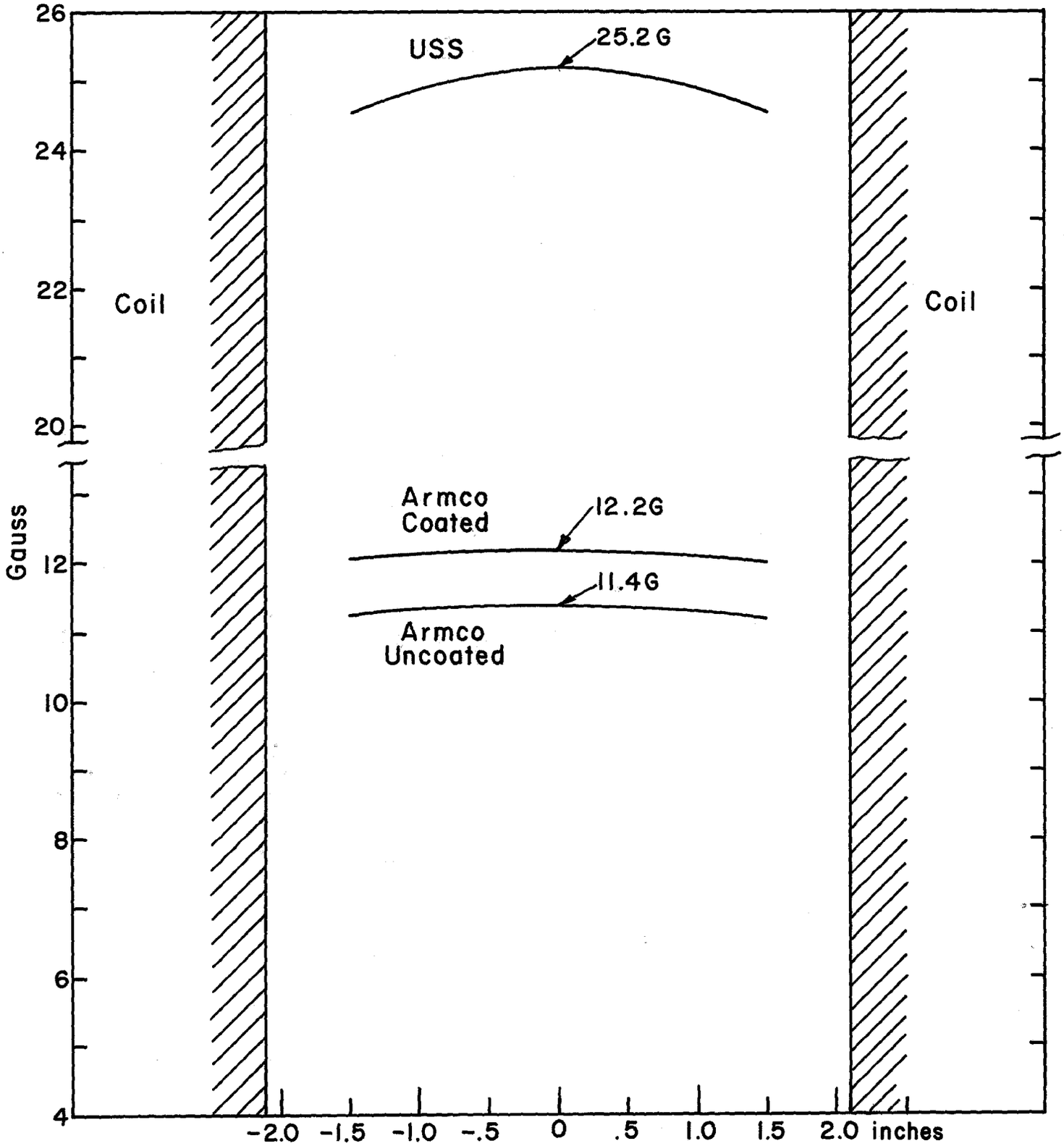

Fig.5 Remanent Field Shapes

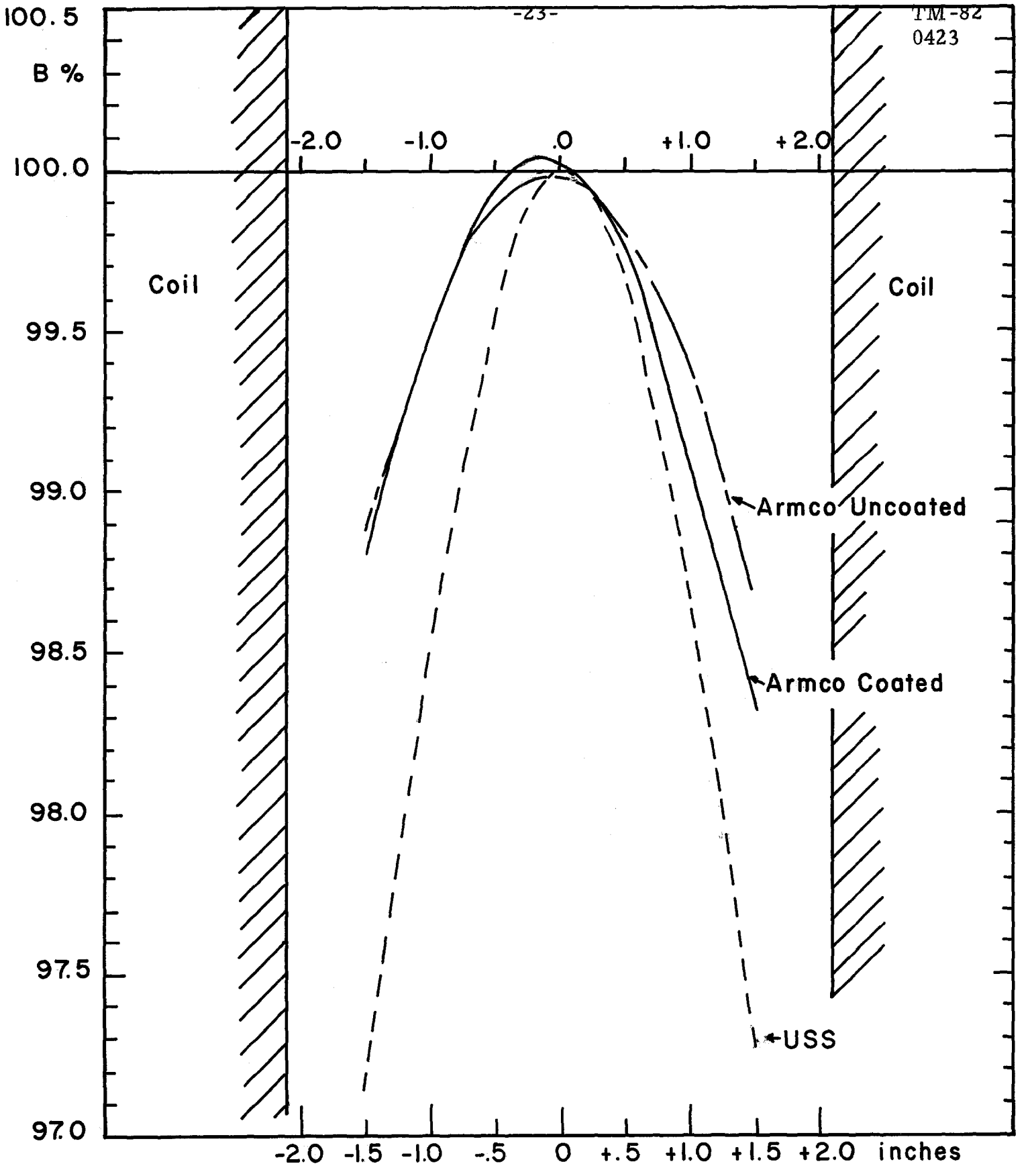

Figure 6 Remanent Field Shapes in Percentage

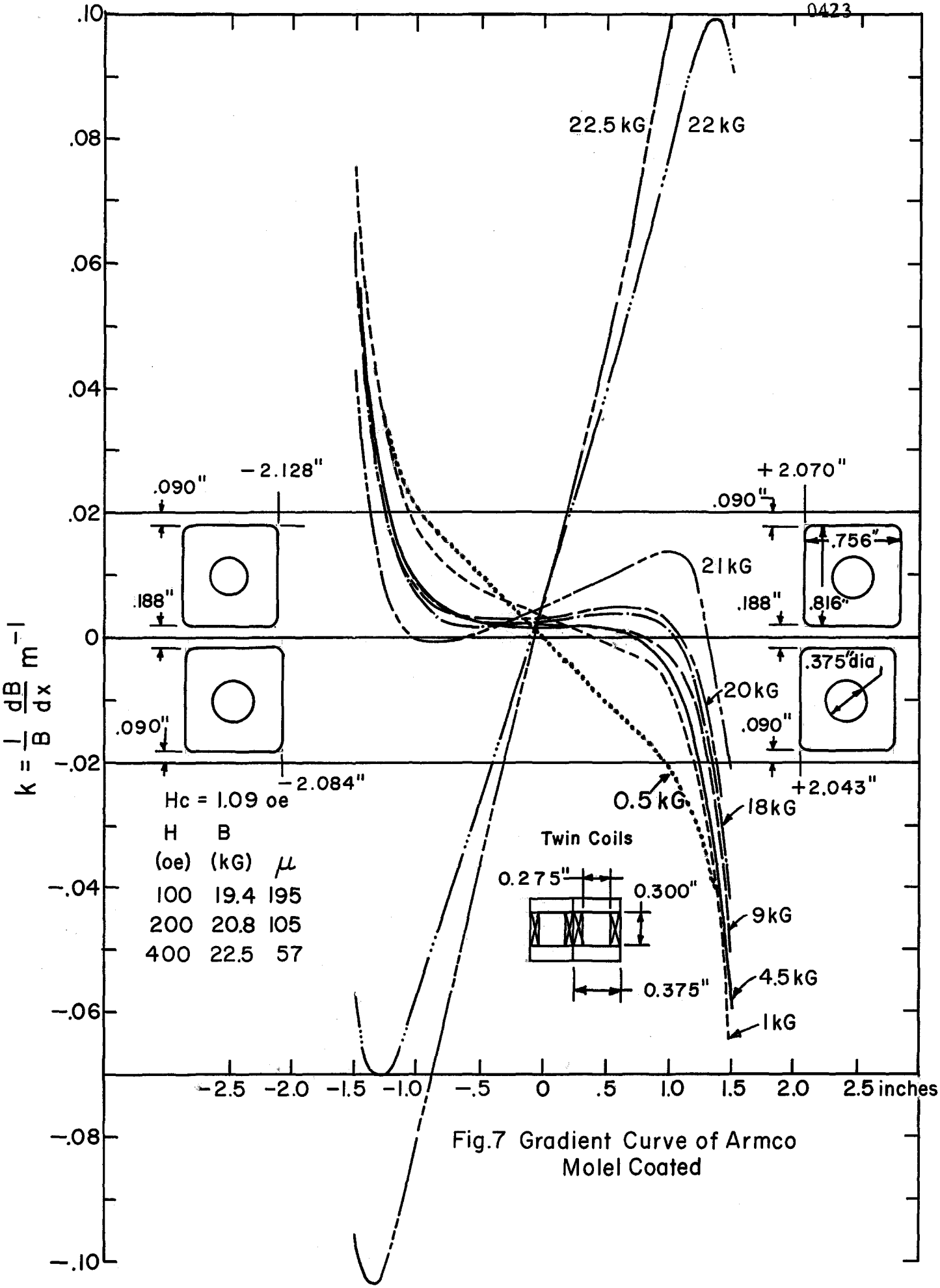

Fig.7 Gradient Curve of Armco Molel Coated

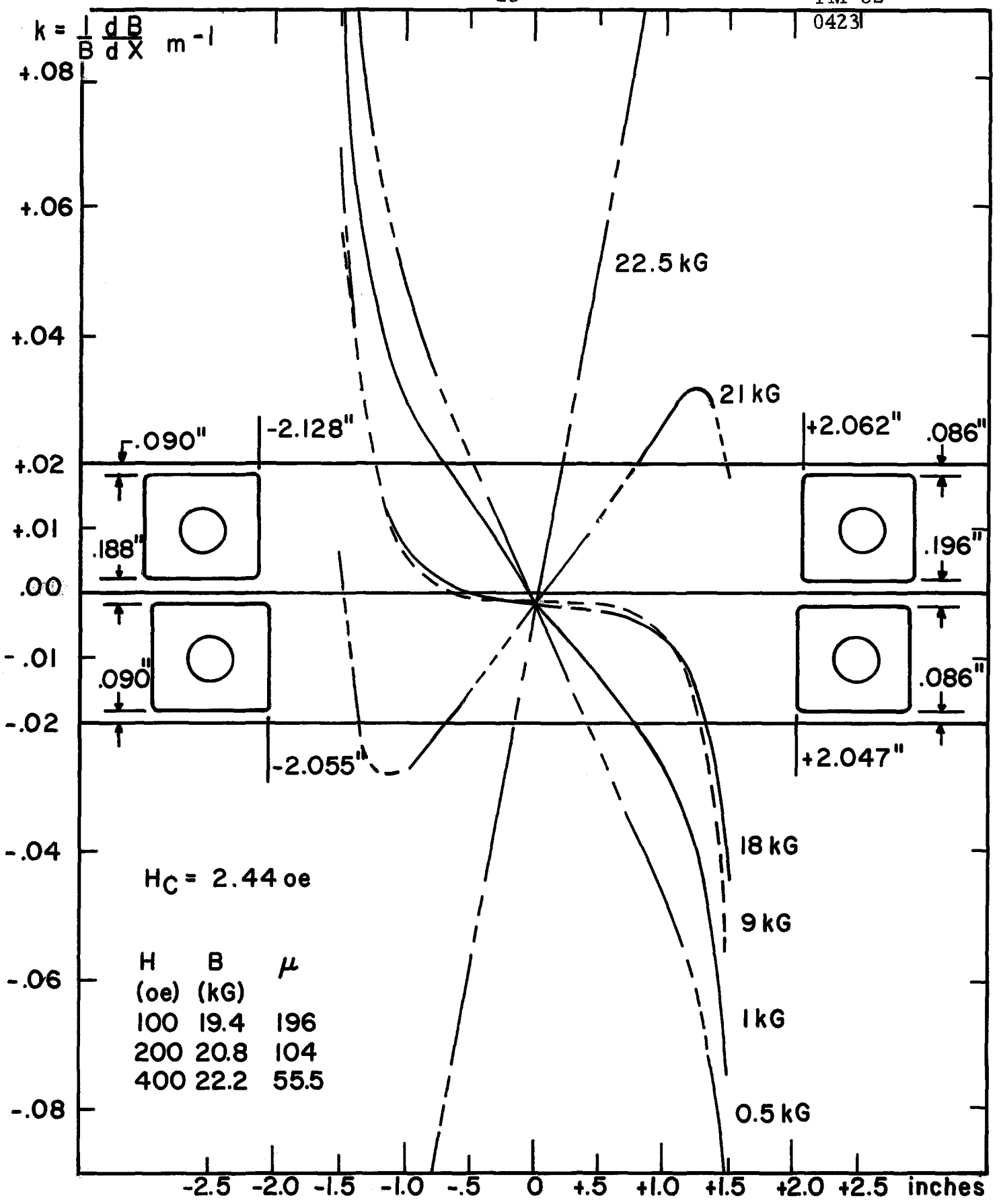

Figure 8 Gradient Curve of USS Vit. I

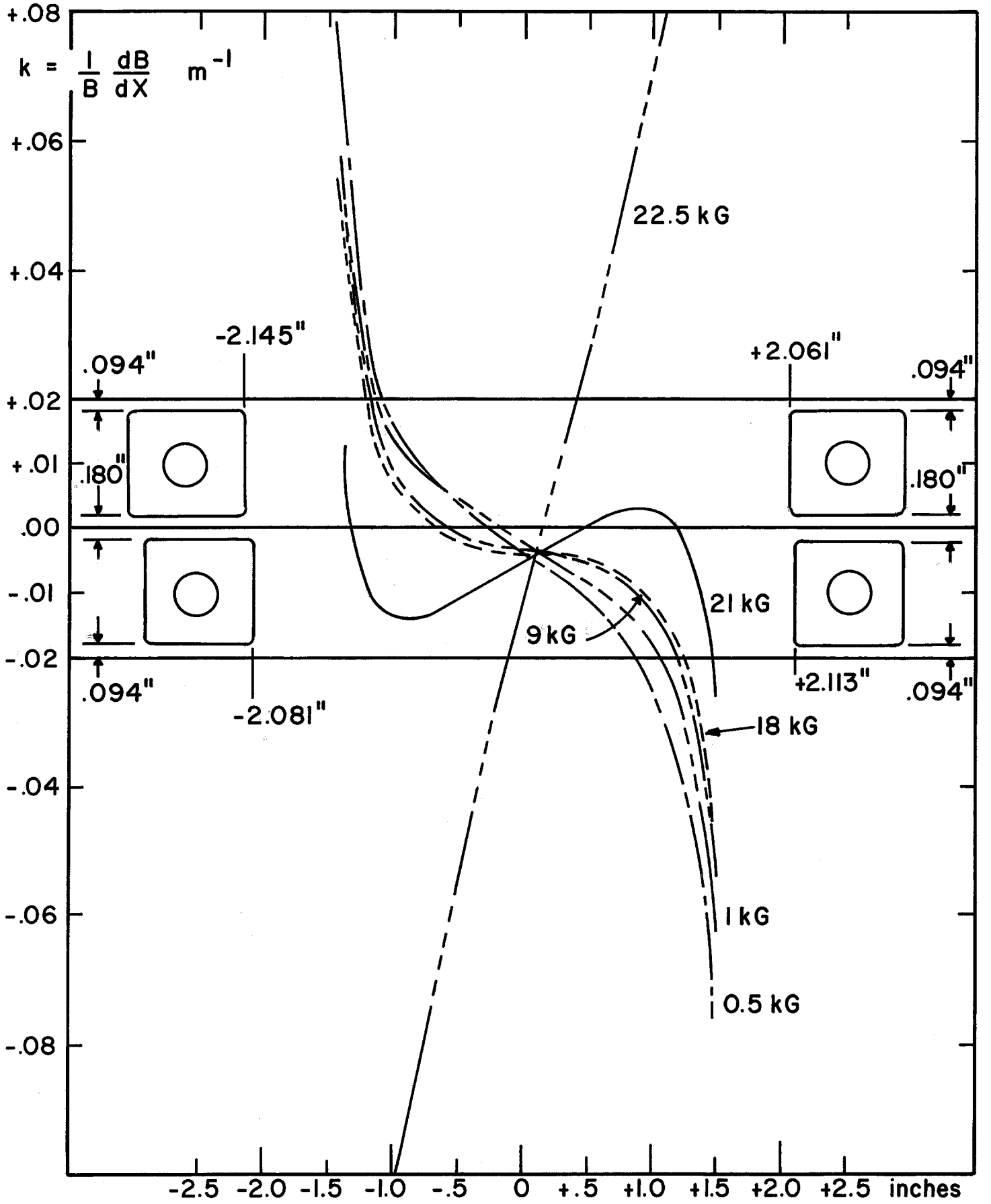

Figure 9 Gradient Curve of Armco Uncoated

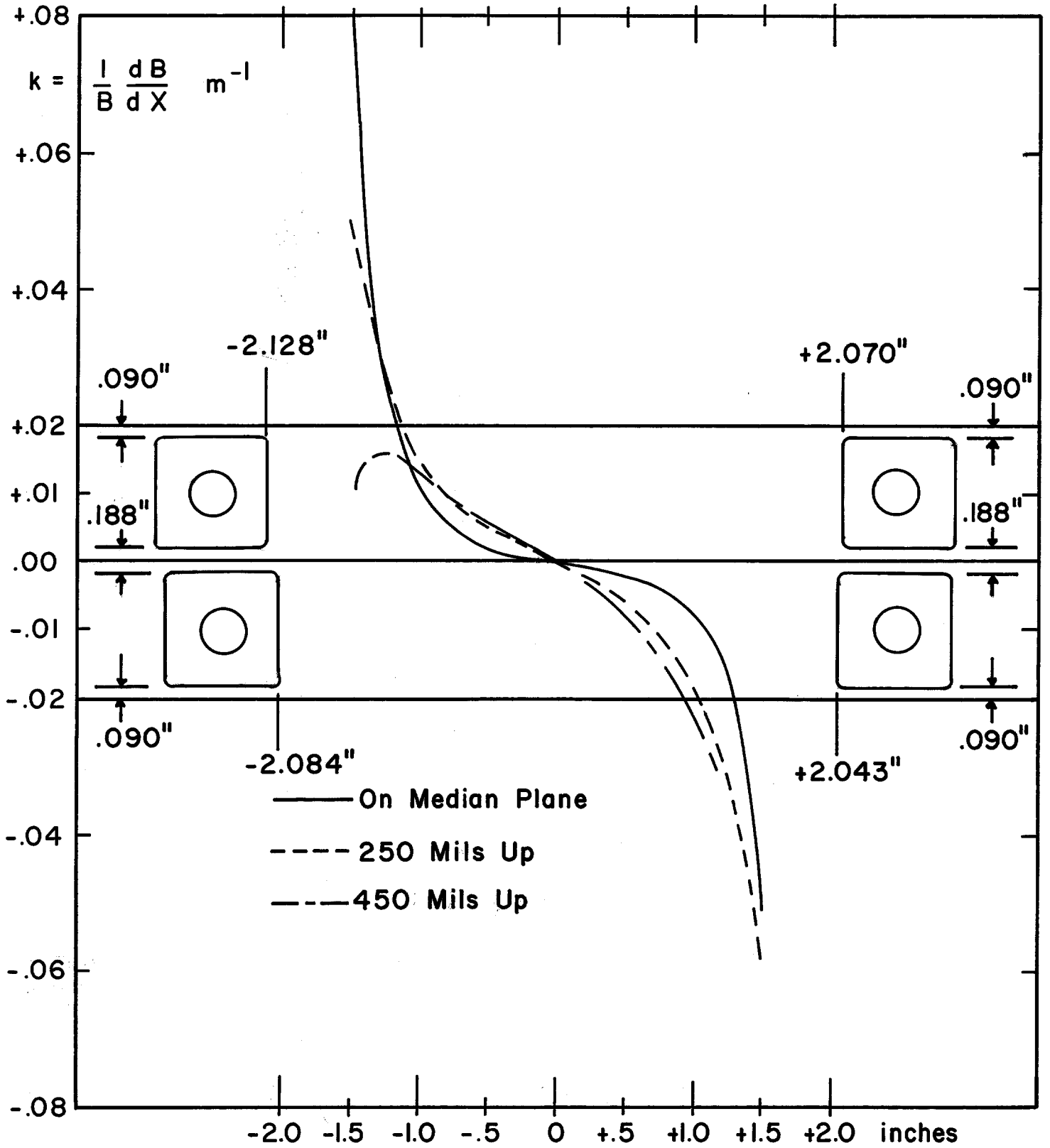

Figure 10 Gradient Curve At Different Height of Armco Coated At 9kG

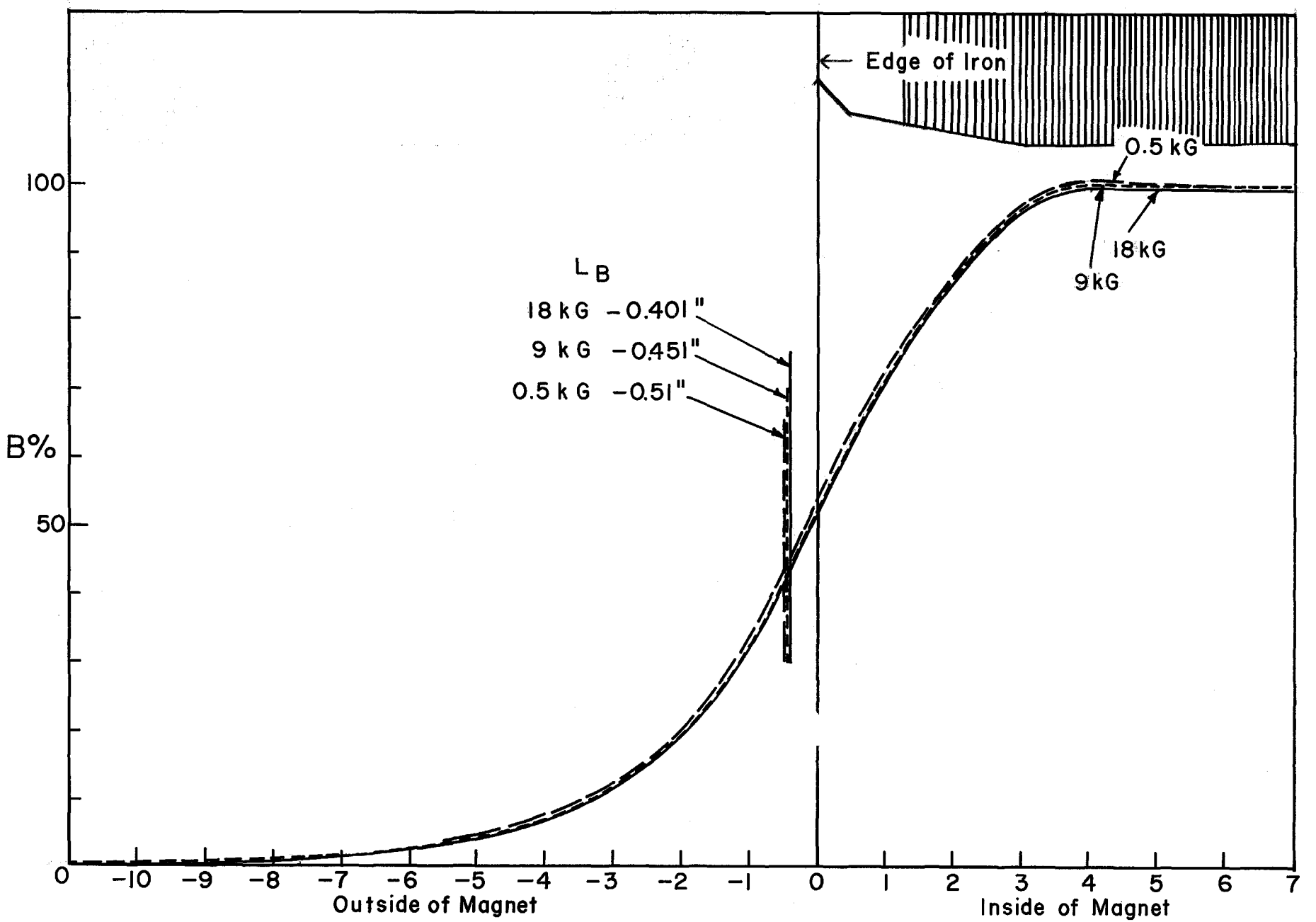

Fig.11 Fringing Field Shape of Two-Step Tapered End

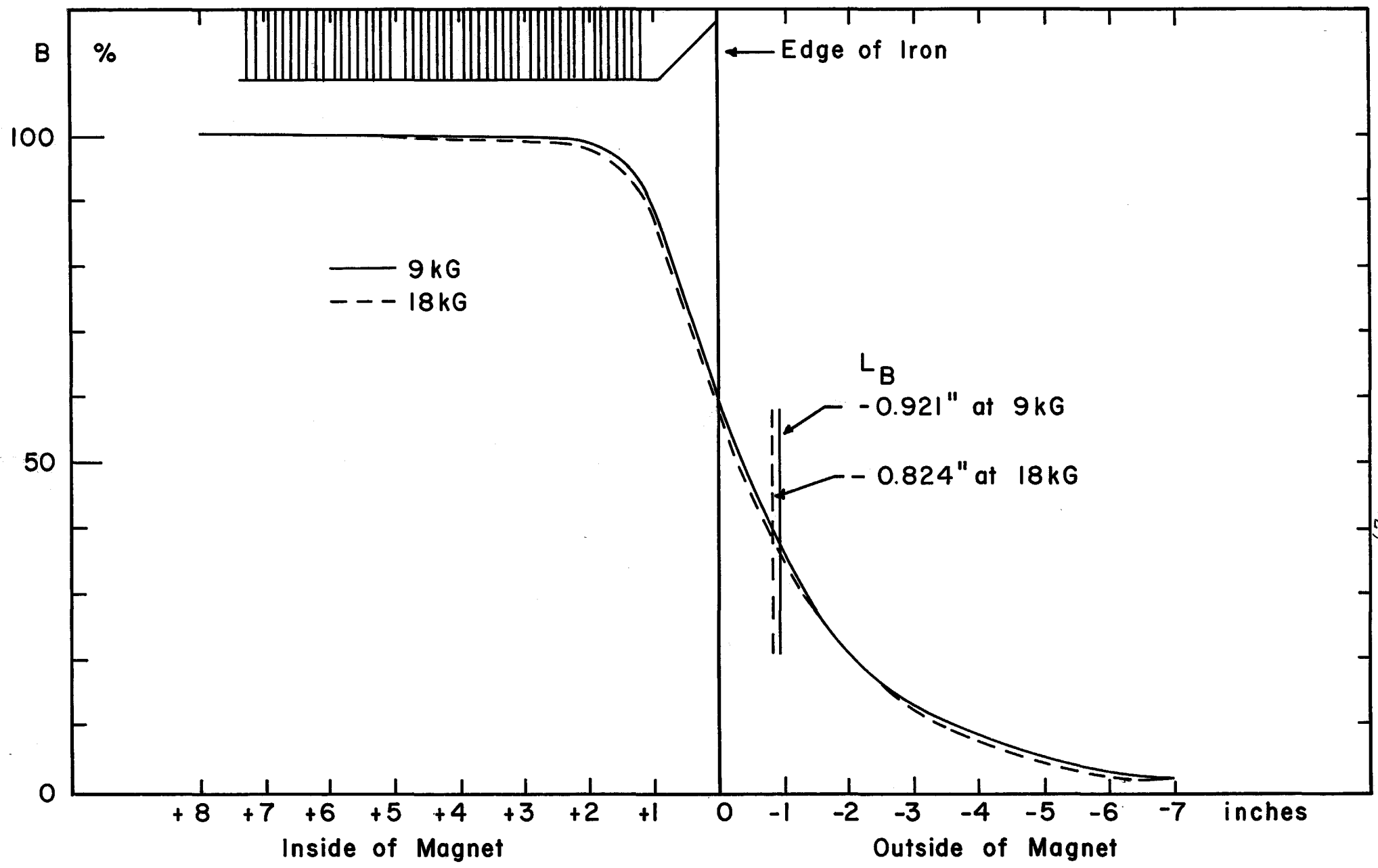

Figure 12 Fringing Field Shape of 45° Tapered End

TM-82
0423

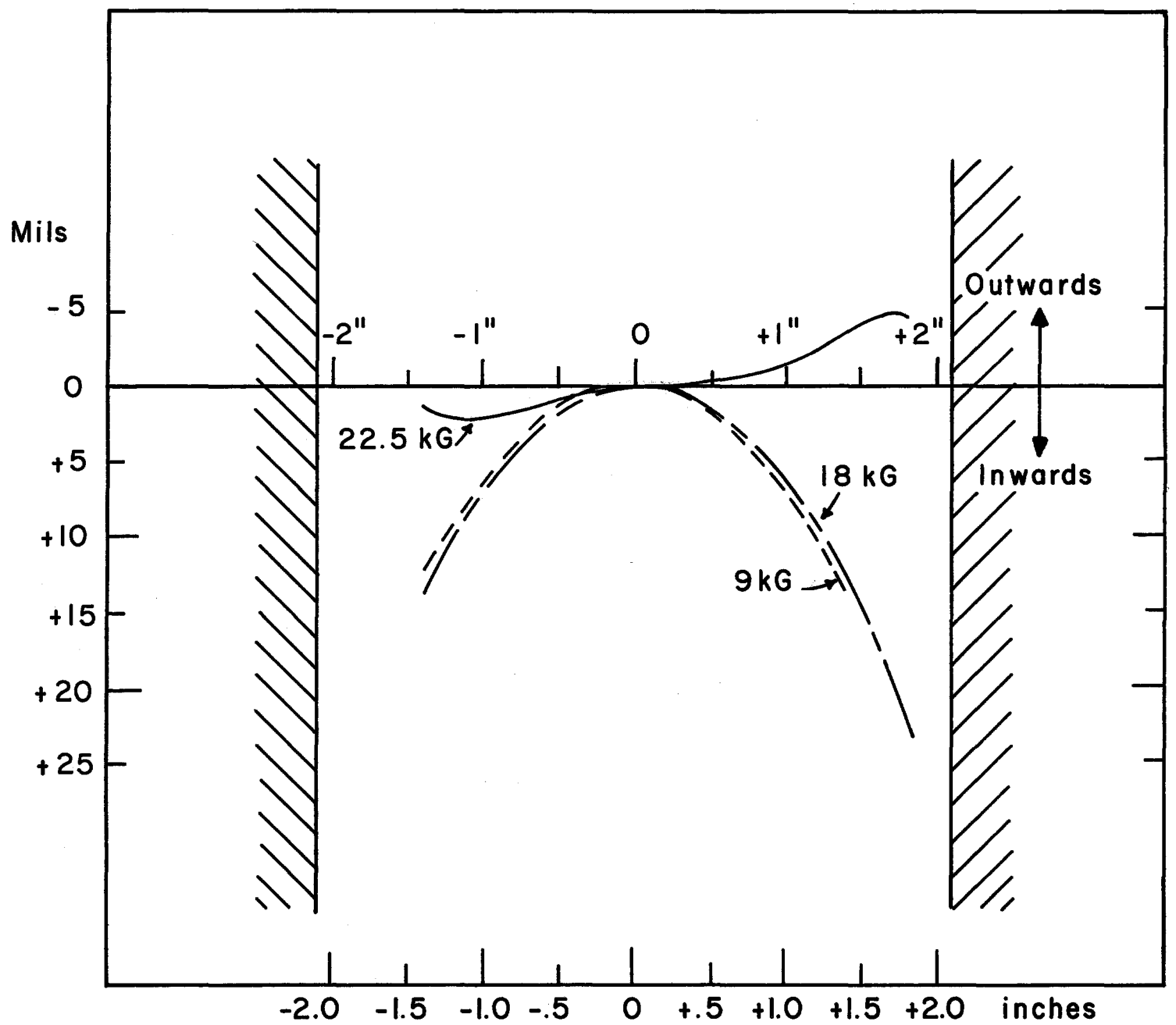

Figure 13 Variation of Effective Magnet Length of Two-Step Tapered End

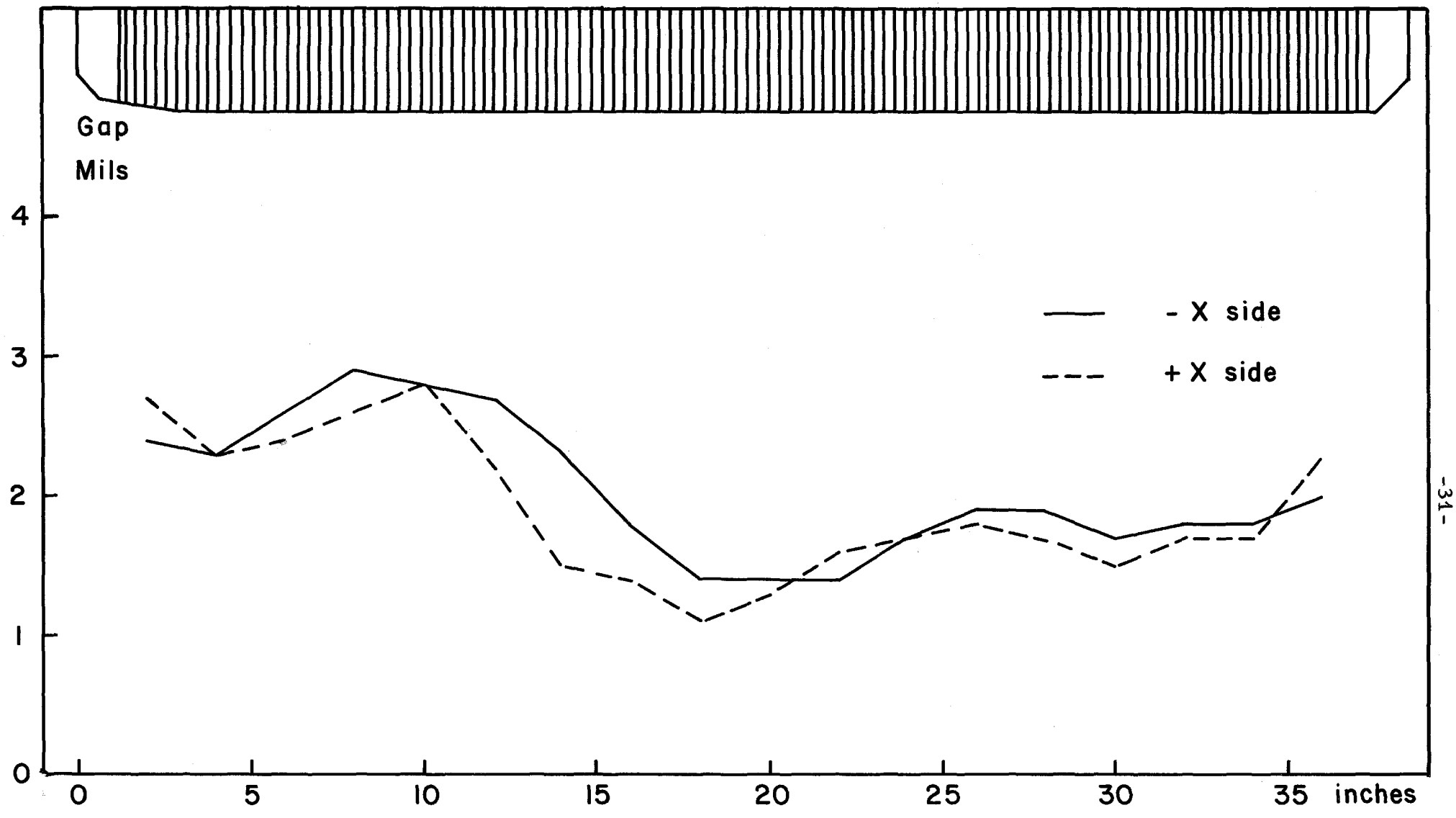

Figure 14 Gap Height Distributions
In Both Back Legs

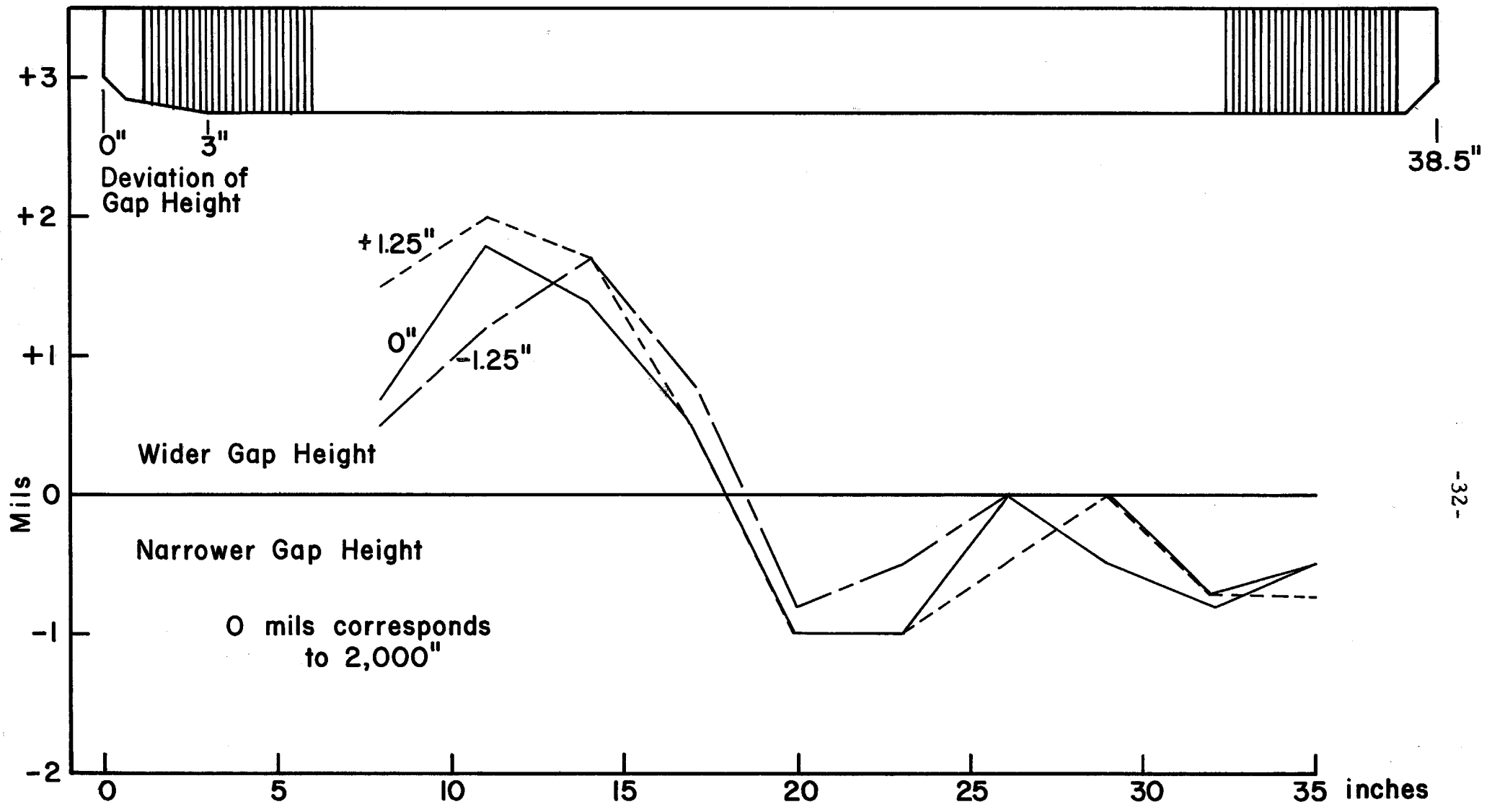

Figure 15 Averaged Gap Height Variation